

RESISTANCE SCALING ON $4N$ -CARPETS

CLAIRE CANNER, CHRISTOPHER HAYES, SHINYU HUANG, MICHAEL ORWIN, AND LUKE G. ROGERS.

ABSTRACT. The $4N$ carpets are a class of infinitely ramified self-similar fractals with a large group of symmetries. For a $4N$ -carpet F , let $\{F_n\}_{n \geq 0}$ be the natural decreasing sequence of compact pre-fractal approximations with $\cap_n F_n = F$. On each F_n , let $\mathcal{E}(u, v) = \int_{F_n} \nabla u \cdot \nabla v dx$ be the classical Dirichlet form and u_n be the unique harmonic function on F_n satisfying a mixed boundary value problem corresponding to assigning a constant potential between two specific subsets of the boundary. Using a method introduced by Barlow and Bass [2], we prove a resistance estimate of the following form: there is $\rho = \rho(N) > 1$ such that $\mathcal{E}(u_n, u_n)\rho^n$ is bounded above and below by constants independent of n . Such estimates have implications for the existence and scaling properties of Dirichlet forms on F .

1. INTRODUCTION

The $4N$ carpets are a class of self-similar fractals related to the classical Sierpiński Carpets. They are defined by a finite set of similitudes with a single contraction ratio, are highly symmetric, and are post-critically infinite. Two examples, the octacarpet ($N = 2$) and dodecacarpet ($N = 3$) are shown in Figure 1. We do not consider the case $N = 1$ which is simply a square.

The construction of $4N$ carpets is as follows; illustrations for $N = 2$ are in Figure 2. Fix $N \geq 2$, let $\Lambda(N) = \{0, \dots, 4N - 1\}$ and $C_j(N) = \exp \frac{(2j-1)i\pi}{4N} \in \mathbb{C}$. Let F_0 denote the convex hull of $\{C_j(N), j \in \Lambda(N)\}$. Consider contractions $\phi_j = r(x - C_j) + C_j$ where the ratio $r = r(N) = (1 + \cot(\pi/4N))^{-1}$ is chosen so $\phi_j(F_0) \cap \phi_k(F_0)$ is a line segment. Let $\Phi(x) = \cup_{j=1}^{4N} \phi_j(x)$ and Φ^n denote the n -fold composition. Then let $F_n = \Phi^n(F_0)$ and $F = \cap_n F_n$ be the unique non-empty compact set such that $\Phi(F) = F$ (see [8]). We call F the $4N$ -carpet. Since one may verify the Moran open set condition is valid for the interior of F_0 , [8, Theorem 5.3(2)] implies its Hausdorff dimension is $d_f = -\log 4N / \log r(N) = \log 4N / \log(1 + \cot(\pi/4N))$.

This paper is concerned by a physically-motivated problem connected to the resistance of the $4N$ carpet, and is closely related to well-known results of Barlow and Bass [2]. To state it we need

2020 *Mathematics Subject Classification.* Primary: 28A80, 31C25, 31E05. Secondary: 31C15, 60J65.

Key words and phrases. Resistance, Fractal, Fractal carpet, Dirichlet form, Walk dimension, Spectral dimension.
Work supported by NSF DMS REU 1659643.

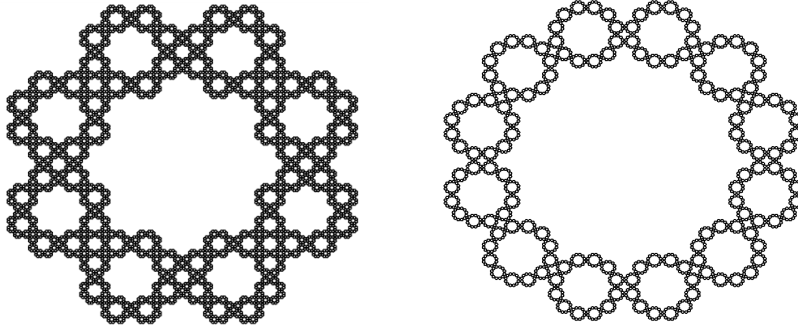
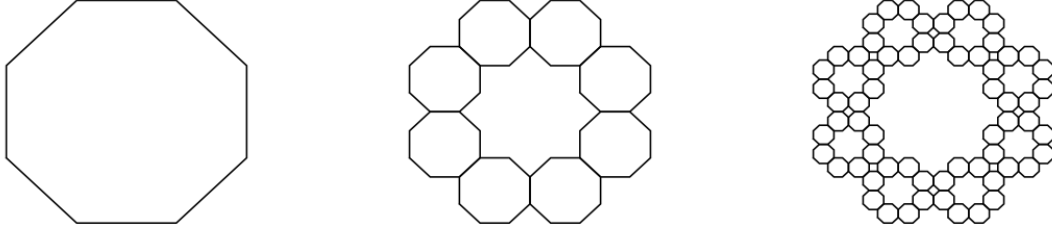


FIGURE 1. The octacarpet ($N = 2$) and dodecacarpet ($N = 3$) are $4N$ -Carpets.

FIGURE 2. The pre-carpet F_0 , F_1 and F_2 for the octacarpet ($N = 2$).

some further notation. Writing subindices modulo $4N$, let L_j be the line segment from C_j to C_{j+1} (these are shown for the case $N = 2$ in the left diagram in Figure 5). Then define

$$(1.1) \quad A_n = F_n \cap \left(\bigcup_{k=0}^{N-1} L_{4k} \right) \quad B_n = F_n \cap \left(\bigcup_{k=0}^{N-1} L_{4k+2} \right)$$

Supposing F_n to be constructed from a thin, electrically conductive sheet let $R_n = R_n(N)$ be the effective resistance (as defined in (2.2) below) when the edges of A_n are short-circuited at potential 1 and those of B_n are short-circuited at potential 0. Bounds for R_n have a well-known connection to exit time estimates for Brownian motion and to proving the existence of and obtaining bounds for the “spectral dimension” of F , as in [3]; they also play a significant role in the Barlow-Bass proof of the existence of Brownian motion on the Sierpiński Carpet and bounds on the associated heat kernel. Although the present work generalizes [2] to the $4N$ -carpets, we do not establish the existence of a Brownian motion. In this connection, we note that the PhD thesis or Ulysses Andrews [1] establishes existence of a Brownian motion on $4N$ -carpets by the Barlow-Bass method under certain assumptions, one of which is that there is a resistance estimate like that in Theorem 1.1. Our main result is the following theorem.

Theorem 1.1. *For fixed $N \geq 2$ there is a constant $\rho = \rho(N)$ such that $\frac{9}{44N} R_0 \rho^n \leq R_n \leq \frac{44N}{9} R_0 \rho^n$.*

Proof. The majority of the work is to establish (in Theorem 4.1 below) that there are constants c, C so $cR_n R_m \leq R_{n+m} \leq CR_n R_m$. Then $S_n = \log cR_n$ is superadditive and $S'_n = \log CR_n$ is subadditive, so Fekete’s lemma implies $\frac{1}{n}S_n \rightarrow \sup \frac{1}{n}S_n$ and $\frac{1}{n}S'_n \rightarrow \inf \frac{1}{n}S'_n$. However $\frac{1}{n}(S_n - S'_n) \rightarrow 0$, so defining $\log \rho$ to be the common limit we conclude $\frac{1}{n}S_n \leq \log \rho \leq \frac{1}{n}S'_n$ and thus $cR_n \leq \rho^n \leq CR_n$. The constants c and C in the stated bound are those from Theorem 4.1. \square

2. RESISTANCE, FLOWS AND CURRENTS

We recall some necessary notions regarding Dirichlet forms on graphs and on Lipschitz domains. Our treatment closely follows [2], which in turn refers to [5] for the graph case.

2.1. Graphs. On a finite set of points G suppose we have $g : G \times G \rightarrow \mathbb{R}$ satisfying for all $x, y \in G$ that $g(x, y) = g(y, x)$, $g(x, y) \geq 0$ and $g(x, x) = 0$. We call g a conductance. It defines a Dirichlet form by

$$\mathcal{E}_G(u, u) = \frac{1}{2} \sum_{x \in G} \sum_{y \in G} g(x, y) (u(x) - u(y))^2.$$

For disjoint subsets A, B from G the effective resistance between them is $R_G(A, B)$ defined by

$$(2.1) \quad R_G(A, B)^{-1} = \inf \{ \mathcal{E}_G(u, u) : u|_A = 0, u|_B = 1 \}.$$

The set of functions in (2.1) are called feasible potentials and the infimum is attained at a unique such potential \tilde{u}_G .

A current from A to B is a function I on the edges of the conductance graph, meaning $I : \{x, y : g(x, y) > 0\} \rightarrow \mathbb{R}$, with properties: $I(x, y) = -I(y, x)$ for all x, y and $\sum_{y \in G} I(x, y) = 0$ if $x \notin A \cup B$. It is called a feasible current if it has unit flux, meaning $\sum_{x \in B} \sum_{y \in G} I(x, y) =$

$-\sum_{x \in A} \sum_{y \in G} I(x, y) = 1$. Note that the first equality is a consequence of the definition of a current. The energy of the current is defined by

$$E_G(I, I) = \frac{1}{2} \sum_{x \in G} \sum_{y \in G} g(x, y)^{-1} I(x, y)^2.$$

Theorem 2.1 ([5, Section 1.3.5]).

$$R_G(A, B) = \inf\{E_G(I, I) : I \text{ is a feasible current}\}.$$

This well-known result is proven by showing that for the optimal potential \tilde{u}_G one may define a current by $\nabla u_G(x, y) = (\tilde{u}_G(y) - \tilde{u}_G(x))g(x, y)$, this current has flux $R_G(A, B)^{-1}$ and the optimal current which attains the infimum in the theorem is $\tilde{I}_G = R_G(A, B)\nabla \tilde{u}_G$.

2.2. Lipschitz domains. The corresponding quantities on a Lipschitz domain $\Omega \subset \mathbb{C}$ may be defined as follows. Suppose A, B are disjoint closed subsets of $\partial\Omega$, write σ for the surface measure on $\partial\Omega$ and ν for the interior unit normal. For $u \in C(\bar{\Omega}) \cap H^1(\Omega)$, the latter being the Sobolev space with one derivative in L^2 , let $\mathcal{E}_\Omega(u, u) = \int_\Omega |\nabla u|^2$ and call u a feasible potential if $u|_A = 0$ and $u|_B = 1$. Then define the effective resistance by

$$(2.2) \quad R_\Omega(A, B)^{-1} = \inf\{\mathcal{E}_\Omega(u, u) : u \text{ is a feasible potential}\}.$$

Now consider a vector field $J : \Omega \rightarrow \mathbb{R}^2$. J is a current between A and B if $J \in BV(\Omega)$ with $\nabla \cdot J = 0$ on Ω in the sense of distributions and $J \cdot \nu = 0$ σ -a.e. on $\partial\Omega \setminus (A \cup B)$. The quantity $\int_A J \cdot \nu d\sigma$ is called the flux through A and the condition $\nabla \cdot J = 0$ and a Gauss-Green integration (e.g. using [6, Theorem 1 of Section 5.8]) gives $\int_B J \cdot \nu d\sigma = -\int_A J \cdot \nu d\sigma$. The current is feasible if both of these fluxes equal 1. Our work here depends crucially on the following result, for which we refer to [4]. It should be noted that this result is not valid for arbitrary mixed boundary value problems on Lipschitz domains; in particular, in [4] it is required that the pieces of the boundary on which the Dirichlet and Neumann conditions hold meet at an angle less than π . This condition will be true for our sets. Alternatively, one can note that our sets have polygonal boundary and therefore the analysis of Grisvard [7, Section 4.3.1] is applicable.

Theorem 2.2. *For the choices of domain Ω and sets A, B considered in this paper, there is a unique $\tilde{u}_\Omega \in C(\bar{\Omega}) \cap H^1(\Omega)$ with $\nabla \tilde{u}_\Omega \in L^2(d\sigma)$ which solves the mixed boundary value problem*

$$\begin{cases} \Delta \tilde{u}_\Omega = 0 & \text{in } \Omega \\ \tilde{u}_\Omega|_A = 0, \tilde{u}_\Omega|_B = 1 \\ \frac{\partial \tilde{u}_\Omega}{\partial \nu} = 0 & \text{a.e. } d\sigma \text{ on } \partial\Omega \setminus (A \cup B). \end{cases}$$

Once this is known, the arguments in [2] directly translate to yield the following analogue of the previously stated result for graphs. It is perhaps worth remarking that the argument uses that $\nabla \tilde{u}_\Omega$ is a current, which requires more regularity on the interior of Ω than simply $\tilde{u}_\Omega \in H^1(\Omega)$, but the required regularity is immediate from $\Delta \tilde{u} = 0$ on Ω .

Theorem 2.3 (See [2, Proposition 2.2 and Theorem 2.3]). *The function \tilde{u}_Ω from Theorem 2.2 is the unique minimizer of (2.2) so satisfies $R_\Omega(A, B)^{-1} = \mathcal{E}_\Omega(\tilde{u}_\Omega, \tilde{u}_\Omega)$. Moreover $\tilde{J}_\Omega = R_\Omega(A, B)\nabla \tilde{u}_\Omega$ is the unique minimizer for $\inf\{E_\Omega(J, J) : J \text{ is a feasible current}\}$ and thus $E_\Omega(\tilde{J}_\Omega, \tilde{J}_\Omega) = R_\Omega(A, B)$.*

3. RESISTANCE ESTIMATES

Suppose Theorem 2.2 is applicable to the Lipschitz domain Ω and disjoint subsets $A, B \subset \partial\Omega$. In light of (2.2) we can bound the resistance from below by $\mathcal{E}_\Omega(u, u)^{-1}$ for u a feasible potential, and by the characterization in Theorem 2.3 we can bound the resistance from above by $E_\Omega(J, J)$ for J a feasible current. To get good resistance estimates one must ensure the potential and current give comparable bounds.

We do this for the pre-carpet sets F_{m+n} following the method of Barlow and Bass in [2]. First we define graphs G_m and D_m , which correspond to scale m approximations of a current and potential (respectively) on F_m , and for which the resistances are comparable. Next we establish the key technical step, which involves using the symmetries of the $4N$ gasket to construct a current with prescribed fluxes through certain sides $L_j \cap F_n$ from the optimal current on F_n (see Proposition 3.8), and to construct a potential with prescribed data at the endpoints of these sides from the optimal potential on F_n (see Proposition 3.10). Combining these results we establish the resistance bounds in Theorem 4.1 by showing that the optimal current on G_m can be used to define a current on F_{m+n} with comparable energy, and the optimal potential on D_m can be used to define a potential on F_{m+n} with comparable energy.

The two symmetries of F and the pre-carpets F_n that play an essential role are the rotation $\theta(z) = ze^{i\pi/2N}$ and complex conjugation. They preserve F and all F_n .

3.1. Graph approximations. For a fixed m the pre-carpet F_m is a union of cells, each of which is a scaled translated copy of the convex set F_0 . We define graphs that reflect the adjacency structure of the cells.

In F_1 , we refer to a cell by the unique vertex C_j it contains. Focusing on the C_0 cell, we identify three sides of significance: the side contained in L_0 , and the sides where the C_0 cell meets the $C_{\pm 1}$ cells. By symmetry under complex conjugation the side where the C_0 and C_1 cells meet is on the real axis. This common side is mapped to the intersection of the C_0 and C_{-1} cells by the rotation θ^{-1} . Recalling the contraction ϕ_0 which maps F_0 to the C_0 cell we conclude that these sides of the C_0 cell are $\phi_0(L_0)$, $\phi_0(L_N)$ and $\phi_0(L_{3N-1})$.

It is straightforward to find a map ψ_j which takes F_0 to the C_j cell in F_1 and has the same adjacency properties we had for the C_0 cell, specifically that $\psi_j(L_0) \subset A_1 \cup B_1$, while $\psi_j(L_N)$ and $\psi_j(L_{3N-1})$ are the sides where the C_j cell intersects the $C_{j\pm 1}$ cells. Using symmetry under complex conjugation and the rotation θ , we see this is achieved by setting

$$\psi_j(z) = \begin{cases} \phi_j \circ \theta^j(z) & \text{if } j \equiv 0 \pmod{2} \\ \phi_j \circ \theta^{j-1}(\bar{z}) & \text{if } j \equiv 1 \pmod{2}. \end{cases}$$

and we also define $\Psi_0 = \cup_j \psi_j : F_0 \rightarrow F_1$.

Observe that for the cells in F_1 we mapped L_0 to the sides of $A_1 \cup B_1$ because these are the sides on which we should specify a voltage or current for our resistance problem. At subsequent levels of the construction things are slightly different. Fix a level m cell and consider mapping F_0 to a level $m+1$ cell within it. As before we arrange that the sides L_N and L_{3N-1} are mapped to the places where the level $m+1$ cells meet their neighbors of the same size. However there can also be adjacency where the level m cell meets its neighbors. Six level $m+1$ cells each contain a single side where there is adjacency to a cell outside their parent m cell, and we want each of these sides to be the image of L_0 under the map of F_0 to the corresponding cell. For other $m+1$ cells we do not care which side is the image of L_0 .

Since the preceding problem involves only scales m and $m+1$ we define the maps as though $m=0$. In this case the required condition is that for each j one has a map $\tilde{\psi}_j$ from F_0 to the C_j cell of F_1 under which $\tilde{\psi}_j(L_N)$ and $\tilde{\psi}_j(L_{3N-1})$ are the sides where the C_j cell intersects the $C_{j\pm 1}$ cells. In addition one wants $\tilde{\psi}_j(L_0) \subset L_0$ if $j \in \{0, 1\}$, $\tilde{\psi}_j(L_0) \subset L_N$ if $j \in \{N, N+1\}$ and $\tilde{\psi}_j(L_0) \subset L_{3N-1}$ if $j \in \{3N-1, 3N\}$. If N is even then $\tilde{\psi}_j = \psi_j$ already has these properties unless $j \in \{3N-1, 3N\}$ where we put $\tilde{\psi}_{3N-1}(z) = \phi_{3N-1} \circ \theta^{3N-1}(z)$ and $\tilde{\psi}_{3N}(z) = \phi_{3N} \circ \theta^{3N-1}(\bar{z})$. Similarly, if N is odd we set $\tilde{\psi}_j = \psi_j$ unless $j \in \{N, N+1\}$ in which case we define $\tilde{\psi}_N(z) = \phi_N \circ \theta^N(z)$ and $\tilde{\psi}_{N+1}(z) = \phi_{N+1} \circ \theta^N(\bar{z})$.

Finally, for a length m word $w = j_1 j_2 \cdots j_m$ we put $\psi_w = \psi_{j_1} \circ \tilde{\psi}_{j_2} \circ \cdots \circ \tilde{\psi}_{j_m}$ and define a map $\Psi_m = \cup_{|w|=m} \psi_w : F_0 \rightarrow F_m$.

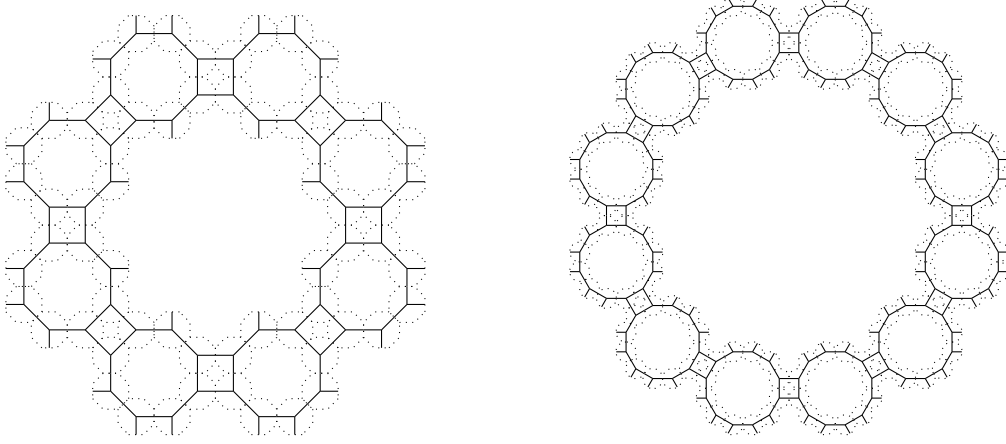


FIGURE 3. The graph approximations G_2 for the octacarpet ($N = 2$) and the dodecacarpet ($N = 3$).

We can now define the graphs G_m that we will use to approximate currents on F_m . They correspond to ignoring the internal structure of cells and recording only the (net) flux through the intersections of pairs of cells. Figure 3 shows such graphs for $n = 2$ on the octacarpet and dodecacarpet.

Definition 3.1. The graph G_0 has vertices at 0 (the center of F_0) and at $\frac{1}{2}(C_j + C_{j+1})$ for $j = 0, N, 3N - 1$ (which are the midpoints of the sides $L_0 \cap F_0$, $L_N \cap F_0$ and $L_{3N-1} \cap F_0$). It has one edge from 0 to each of the other three vertices. The graphs G_m are defined via $G_m = \Psi_m(G_0)$.

Let \tilde{I}_m^G be the optimal current from A_m to B_m on G_m ; by symmetry the flux through each vertex in A_m is then $-\frac{2}{N}$ and that through each vertex in B_m is $\frac{2}{N}$, giving unit flux from A_m to B_m ; these sets were defined in (1.1). The corresponding optimal potential is denoted \tilde{u}_m^G and is 0 on A_m and 1 on B_m . We write R_m^G for the resistance of G_m defined as in (2.1). Also note that $\tilde{I}_m^G \circ \psi_w$ is a current on G_0 for each word w of length m .

The graphs D_m that we use to approximate potentials on F_m have vertices at each endpoint of a side common to two cells. Figure 4 shows the first few D_n for $N = 2$ and $N = 3$.

Definition 3.2. The graph D_0 has vertices $\{0, C_0, C_1, C_N, C_{N+1}, C_{3N-1}, C_{3N}\}$ and edges from 0 to each of the other six vertices. The graphs D_m are defined by $\Psi_m(D_0)$. Figure 4 shows these graphs for $n = 0, 1, 2$ on the octacarpet and dodecacarpet.

We let \tilde{u}_m^G denote the optimal potential on D_m for the boundary conditions $\tilde{u}_m = 0$ at vertices in A_m and $\tilde{u}_m = 1$ at vertices in B_m . The resistance of D_m is written R_m^D . As for currents, $\tilde{u}_m \circ \psi_w$ is a potential on D_0 for any word w of length m .

Lemma 3.3. For all $m \geq 1$, $R_m^G = 2R_m^D$.

Proof. Each edge in G_m connects the center x of a cell to a point y on a side of the cell. Writing y_{\pm} for the endpoints of that side we see that there are two edges in D_m connecting x to the same side at y_{\pm} . In this sense, each edge of G_m corresponds to two edges of D_m and conversely.

From the optimal potential \tilde{u}_m^G for G_m define a function f on D_m by setting $f(x) = \tilde{u}_m^G(x)$ at cell centers and $f(y_{\pm}) = \tilde{u}_m^G(y)$ at endpoints y_{\pm} of a side with center y . This ensures $f(y_{\pm}) - f(x) = \tilde{u}_m^G(y) - \tilde{u}_m^G(x)$, so that two edges in D_m have the same edge difference as the corresponding single edge in G_m . Clearly f is a feasible potential on D_m , so $(R_m^D)^{-1} \leq \mathcal{E}_{D_m}(f, f) = 2\mathcal{E}_{G_m}(\tilde{u}_m^G, \tilde{u}_m^G) = 2(R_m^G)^{-1}$.

Conversely, beginning with the optimal potential \tilde{u}_m^D define f on G_m by $f(x) = \tilde{u}_m^D(x)$ at cell centers and $f(y) = \frac{1}{2}(\tilde{u}_m^D(y_+) + \tilde{u}_m^D(y_-))$ if y is the center of a cell side with endpoints y_{\pm} . The edge

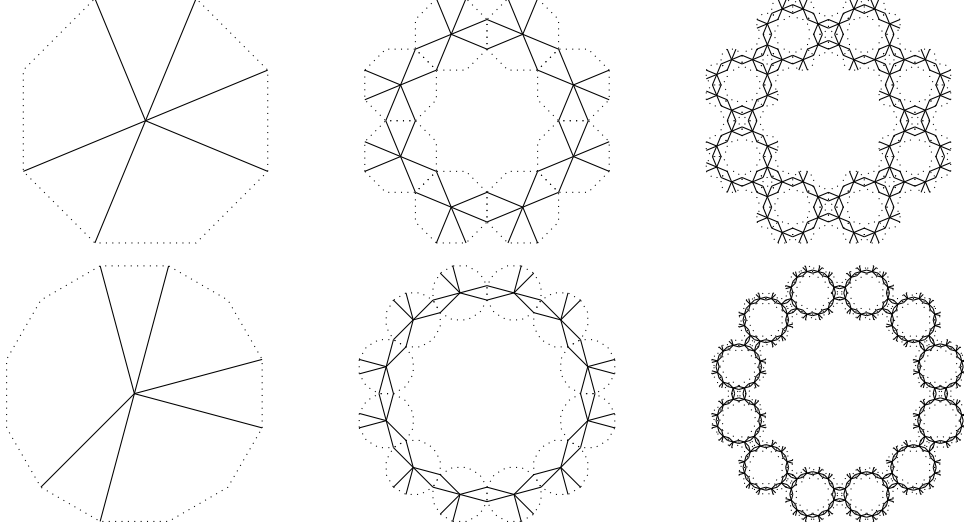


FIGURE 4. The graph approximations D_0 , D_1 and D_2 for the octacarpet ($N = 2$) and the dodecacarpet ($N = 3$). Note that D_0 corresponds with the sides L_0 , L_N , and L_{3N-1} , whereas D_1, D_2 correspond with $A_1 \cup B_1$ and $A_2 \cup B_2$.

difference $f(x) - f(y)$ in G_m is half the sum of the edge difference on the corresponding edges in D_m , so using that f is a feasible potential on G_m we have $(R_m^G)^{-1} \leq \mathcal{E}_{G_m}(f, f) = \frac{1}{2} \mathcal{E}_{D_m}(\tilde{u}_m^G, \tilde{u}_m^G) = \frac{1}{2} (R_m^D)^{-1}$. \square

3.2. Currents and potentials with energy estimates via symmetry. Fix $n \geq 0$ and recall that \tilde{u}_{F_n} denotes the optimal potential on F_n with boundary values 0 on A_n and 1 on B_n . In order to exploit the symmetries of F_n it is convenient to work instead with $u_n = 2\tilde{u}_{F_n} - 1$; evidently $\mathcal{E}_{F_n}(u_n, u_n) = 4\mathcal{E}_{F_n}(\tilde{u}_{F_n}, \tilde{u}_{F_n}) = 4R_n^{-1}$ is then minimal for potentials that are -1 on A_n and 1 on B_n . The corresponding current $J_n = R_n \nabla u_n$ minimizes the energy for currents with flux 2 from A_n to B_n and has $E_{F_n}(J_n, J_n) = 4R_n$. We begin our analysis by recording some symmetry properties of J_n .

Lemma 3.4. *Both $u_n \circ \theta^2 = -u_n$ and $J_n \circ \theta^2 = -J_n$.*

Proof. The rotation θ takes C_j to C_{j+1} , thus L_j to L_{j+1} . It then follows from the definition (1.1) of A_n and B_n that θ^2 exchanges A_n and B_n . Since the optimal potential u_n and current J_n are determined by their boundary data on A_n and B_n this gives the result. \square

One consequence of this lemma is that the flux of J_n through each of the sides $L_j \cap F_n$ in A_n is independent of j and hence equal to $-\frac{2}{N}$. Similarly, the flux through each side in B_n is $\frac{2}{N}$.

Lemma 3.5. *Both $u_n(\bar{z}) = u_n(z)$ and $J_n(\bar{z}) = J_n(z)$.*

Proof. Under complex conjugation the point $C_j = \exp \frac{(2j-1)i\pi}{4N}$ is mapped to

$$\bar{C}_j = \exp \frac{(1-2j)i\pi}{4N} = \exp \frac{(8N-2j+1)i\pi}{4N} = \exp \frac{(2(4N-j+1)-1)i\pi}{4N} = C_{4N-j+1}$$

Then the endpoints C_{4k} and C_{4k+1} of L_{4k} are mapped to $C_{4(N-k)+1}$ and $C_{4(N-k)}$ so L_{4k} is mapped to $L_{4(N-k)}$. This shows A_n is invariant under complex conjugation. Similarly, $\bar{C}_{4k+2} = C_{4(N-k-1)+3}$ and $\bar{C}_{4k+3} = C_{4(N-k-1)+2}$, so L_{4k+2} is mapped to $L_{4(N-k-1)}$ and B_n is invariant under complex conjugation. Both u_n and J_n are determined by their boundary data on these sets. \square

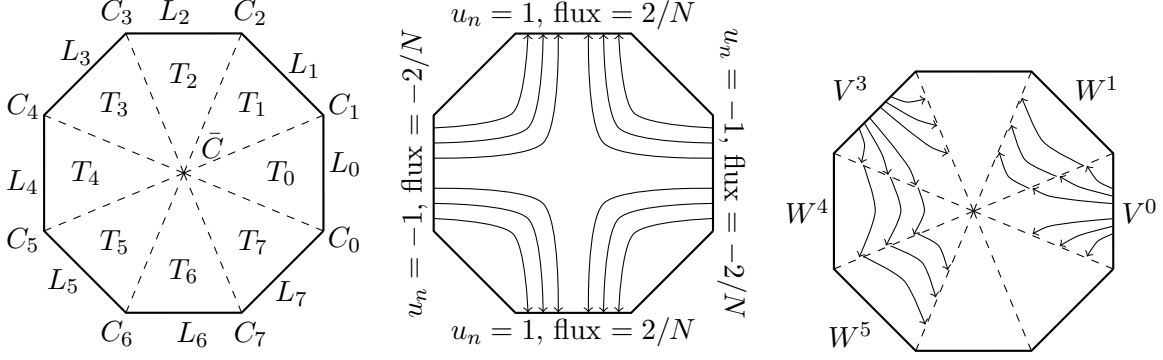


FIGURE 5. For $N = 2$: Decomposition of F_0 into triangles T_j (left), General current flow lines for J_n (middle), and examples of V^j and W^j vector fields (right)

We decompose F_n into triangles by taking, for integers j and $j + 1$ modulo $4N$, T_j to be the interior of the triangle with vertices $\{0, C_j, C_{j+1}\}$. This is shown for $N = 2$ in the left image in Figure 5. Then the central diagram in Figure 5 illustrates the fact that, up to a change of sign, both u_n and J_n have one behavior on triangles T_j with j even, and another behavior on triangles with j odd. This motivates us to define

$$(3.1) \quad v^j = (u_n \circ \theta^{-j})|_{T_j} \quad w^j = (u_n \circ \theta^{-j+1})|_{T_j}$$

$$(3.2) \quad V^j = (J_n \circ \theta^{-j})|_{T_j} \quad W^j = (J_n \circ \theta^{-j+1})|_{T_j}.$$

Examples of V^j and W^j on triangles T_1 and T_4 are shown on the right in Figure 5 for $N = 2$.

Symmetry under rotations shows us that the following quantities are independent of j

$$(3.3) \quad \mathcal{E}_n(v) = \int_{T_j} |v^j|^2 \quad \mathcal{E}_n(w) = \int_{T_j} |w^j|^2$$

$$(3.4) \quad E_n(V) = \int_{T_j} |V^j|^2 \quad E_n(W) = \int_{T_j} |W^j|^2$$

and therefore that

$$(3.5) \quad 4R_n^{-1} = \mathcal{E}_{F_n}(u_n, u_n) = 2N(\mathcal{E}_n(v) + \mathcal{E}_n(w))$$

$$(3.6) \quad 4R_n = E_{F_n}(J_n, J_n) = 2N(E_n(V) + E_n(W)).$$

Lemma 3.6. For any $j \in \Lambda(N)$, $\int_{T_j} \nabla v^j \cdot \nabla w^j = \int_{T_j} V^j \cdot W^j = 0$.

Proof. By rotational symmetry it is enough to verify this for $j = 0$. Since $J_n = R_n u_n$, we have $\nabla v^j = R_n V^j$ and $\nabla w^j = R_n W^j$, so we work only with V^0 and W^0 . The triangle T_0 is symmetrical under complex conjugation, and using Lemmas 3.4 and 3.5 we have

$$(3.7) \quad V^0(\bar{z}) = J_n(\bar{z}) = J_n(z) = V^0(z),$$

$$(3.8) \quad W^0(\bar{z}) = J_n \circ \theta(\bar{z}) = -J_n \circ \theta^{-1}(\bar{z}) = -J_n(\overline{\theta(z)}) = -J_n(\theta(z)) = -W^0(z).$$

Thus $V^0 \cdot W^0(\bar{z}) = -V^0 \cdot W^0(z)$ and the result follows. \square

In addition to being orthogonal, the vector fields V^j and W^j have the property that they can easily be glued together to form currents on F_n . Recall that to be a current a vector field J of bounded variation must have $\nabla \cdot J = 0$.

Lemma 3.7. If J is a vector field such that $J|_{T_l} = \alpha_l V^l + \beta_l W^l$ and $\alpha_{l+1} + \alpha_l = \beta_{l+1} - \beta_l$ for each l , then J is a current.

Proof. The fields V^l and W^l are currents, so are of bounded variation and zero divergence on T_l . It follows that the field is of bounded variation on F_n by the argument of [6, Theorem 1 of Section 5.4]. Moreover, a small modification of the proof of that theorem, together with the Gauss-Green theorem [6, Theorem 1 of Section 5.8] shows that the divergence on the radial line common to the boundaries of T_l and T_{l+1} is the sum of the oriented fluxes through these surfaces, times the linear measure. It is perhaps worth noting that since T_l and T_{l+1} are open, the fields are actually not defined (pointwise) on this common side, but this is of no significance because they are distributions.

The symmetry of V^0 in (3.7) shows the fluxes of V^0 and $-V^1$ cancel on $T_0 \cap T_1$, so $V^0 - V^1$ is a current on $T_0 \cup T_1$. Similarly, the antisymmetry of W^0 in (3.8) shows the fluxes of W^0 and W^1 cancel on $T_0 \cap T_1$, so $W^0 + W^1$ is a current on $T_0 \cup T_1$. In addition we note that $V^1 + W^1 = J_n|_{T_0 \cup T_1}$ is the restriction of the optimal current and is hence a current on $T_0 \cup T_1$. Combining these with the definition (3.2) we see that each of $V^l - V^{l+1}$, $W^l + W^{l+1}$ and $V^l + W^{l+1}$ are currents on $T_l \cup T_{l+1}$ as they are obtained from the $l = 0$ case by rotations.

The divergence of J then vanishes on $T_l \cap T_{l+1}$ by writing $J|_{T_l \cup T_{l+1}}$ as the linear combination $-\alpha_{l+1}(V^l - V^{l+1}) + \beta_l(W^l + W^{l+1}) + (\alpha_l + \alpha_{l+1})(V^l + W^{l+1})$. \square

We will need currents with specified non-zero fluxes on the three sides at which cells join and zero flux on the other sides. The relevant sides were determined in Section 3.1; they are those which contain a vertex of G_0 .

Proposition 3.8. *If I_j , $j = 0, N, 3N - 1$ satisfy $\sum_{0, N, 3N-1} I_j = 0$ then there is a current J on F_n with flux I_j on $L_j \cap F_n$ for $j = 0, N, 3N - 1$ and zero on all other $L_j \cap F_n$ and that has energy*

$$E_{F_n}(J, J) \leq \left(\frac{N^2}{4} E(V) + \frac{N^2}{18} (11N - 8) E(W) \right) \sum_{0, N, 3N-1} I_j^2 \leq \frac{11}{9} N^2 R_n \sum_{0, N, 3N-1} I_j^2$$

Proof. Write $\Lambda'(N) = \{0, N, 3N - 1\}$. Define coefficients β_j by

$$\beta_j = \begin{cases} I_N - I_{3N-1} & \text{if } j = 0 \\ I_{3N-1} - I_0 & \text{if } j = N \\ I_0 - I_N & \text{if } j = 3N - 1 \end{cases} \quad \beta_j = \begin{cases} 2I_N - 2I_0 & \text{if } 1 \leq j \leq N - 1 \\ 2I_{3N-1} - 2I_N & \text{if } N + 1 \leq j \leq 3N - 2 \\ 2I_0 - 2I_{3N-1} & \text{if } 3N \leq j \leq 4N - 1 \end{cases}$$

and let

$$J = -\frac{N}{2} \sum_{j \in \Lambda'} I_j V^j + \frac{N}{6} \sum_{j \in \Lambda} \beta_j W^j.$$

Then J is of the form $\sum_j \alpha_j V^j + \beta_j W^j$ with $\alpha_j = -\frac{N}{2} I_j$ for $j \in \Lambda'$ and zero otherwise. One can verify the conditions of Lemma 3.7, so J is a current. Moreover, all of the W^j have zero flux through $L_j \cap F_n$, and V^j has flux $-\frac{2}{N}$ through $L_j \cap F_n$, thus the flux of J is as stated.

By the orthogonality in Lemma 3.6 and (3.4),

$$E_{F_n}(J, J) = \frac{N^2}{4} E(V) \sum_{\Lambda'} I_j^2 + \frac{N^2}{36} E(W) \sum_{\Lambda} \beta_j^2.$$

It is straightforward to compute

$$\begin{aligned} \sum_{\Lambda} \beta_j^2 &= (4N - 3)(I_N - I_0)^2 + (8N - 7)(I_{3N-1} - I_N)^2 + (4N + 1)(I_0 - I_{3N-1})^2 \\ &= (16N - 9)I_0^2 + (20N - 17)I_N^2 + (20N - 13)I_{3N-1}^2 + 4(N - 1)I_0 I_N + 4(N - 2)I_0 I_{3N-1} \end{aligned}$$

where we used $-2I_N I_{3N-1} = I_0^2 + I_N^2 + I_{3N-1}^2 + 2I_0 I_N + 2I_0 I_{3N-1}$, which was obtained by squaring $\sum_{\Lambda'} I_j = 0$. Then the bound $2I_0 I_j \leq \frac{3}{2}I_0^2 + \frac{2}{3}I_j^2$ for $j = N, 3N-1$ gives, also using $N \geq 2$,

$$\sum_{\Lambda} \beta_j^2 \leq (22N-18)I_0^2 + (22N-19)I_N^2 + (22N-16)I_{3N-1}^2.$$

This gives the energy estimate. The bound by R_n is from the expression following (3.4). \square

Having established these results on currents, we turn to considering potentials, which will be built from the functions v^j and w^j so as to have specified boundary data at those C_j which are vertices of the graph D_0 from Section 3.1.

Lemma 3.9. *The function $v^1 + w^1 + v^0 - w^0$ extends continuously to F_n .*

Proof. In what follows we abuse notation to say a function is continuous on a union of the T_j if it has continuous extension to the closure of this union.

The proof uses the symmetries $v^0(\bar{z}) = v^0(z)$ and $w^0(\bar{z}) = -w^0(z)$, which follow from Lemma 3.5 in the same manner as the proofs of (3.7) and (3.8). Note that $z \mapsto \theta(\bar{z})$ is an isometry of $T_0 \cup T_1$ and compute from the symmetries and (3.1) that

$$(3.9) \quad \begin{aligned} v^0(\theta(\bar{z})) &= v^0(\theta^{-1}(z)) = v^1(z), \\ w^1(\theta(\bar{z})) &= w^0(\bar{z}) = -w^0(z). \end{aligned}$$

Now observe that $v^0 + w^1$ is continuous on $T_0 \cup T_1$ because it is the restriction of the optimal potential u_n to this set, see (3.1). Using the preceding it follows that $(v^1 - w^0)(z) = (v^0 + w^1)(\theta(\bar{z}))$ is also continuous, and thus $v^1 + w^1 + v^0 - w^0$ is continuous on $T_0 \cup T_1$. What is more, we see that if z is in the common boundary of T_0 and T_1 then $\theta(\bar{z}) = z$ and thus (3.9) gives $w^1(z) = -w^0(z)$. Continuity of $v^0 + w^1$ at such points then implies $v^0(z) = -w^0(z)$, but this says $v^0 + w^0$ vanishes identically on the common boundary of T_0 and T_1 . Thus $v^1 + w^1 = v^0 + w^0 \circ \theta^{-1}$ vanishes on the common boundary of T_1 and T_2 , and $(v^0 - w^0)(z) = (v^0 + w^0)(\bar{z})$ vanishes on the common boundary of T_0 and T_{-1} . Together these show $v^1 + w^1 + v^0 - w^0$ vanishes on the boundary of $T_0 \cup T_1$ in F_n , completing the proof. \square

Proposition 3.10. *Given a function u on D_0 that is harmonic at 0 there is a potential f on F_n with $f(C_j) = u(C_j)$ for $C_j \in D_0$ and*

$$\mathcal{E}_{F_n}(f, f) \leq (\mathcal{E}_n(v) + \mathcal{E}_n(w)) \sum_{C_j \in D_0} (u(C_j) - u(0))^2 = \frac{2}{N} R_n^{-1} \sum_{C_j \in D_0} (u(C_j) - u(0))^2.$$

If $f(C_{j+1}) = f(C_j)$ for some $j \in \{0, N, 3N-1\}$ then f is constant on the edge $L_j \cap F_n$.

Proof. Let $z_j = u(C_j) - u(0)$ for $C_j \in D_0$ and $z_j = 0$ otherwise. With indices modulo $4N$, define

$$f = u(0) + \frac{1}{2} \sum_{j \in \Lambda(N)} z_j (w^{j-1} - v^{j-1} - v^j - w^j) = u(0) + \frac{1}{2} \sum_j (z_{j+1} - z_j) w^j - (z_{j+1} + z_j) v^j.$$

This is continuous on F_n because it is a linear combination of rotations of the function in Lemma 3.9. Recall from Section 2.2 that a function is a potential if it is continuous and in the Sobolev space H^1 . Since v^j and w^j are restrictions of Sobolev functions to the domains T_j , it is standard that a linear combination which extends to be continuous on $\cup_j T_j$ is Sobolev on $\cup_j T_j$; for example it follows immediately from the characterization of H^1 using absolute continuity on lines, see [9, Theorem 2.1.4]. We therefore conclude that f is a potential. Using $w^{j-1}(C_j) = 1$, $v^{j-1}(C_j) = w^{j-1}(C_j) = w^j(C_j) = -1$ and $v^l(C_j) = w^l(C_j) = 0$ for $l \neq j, j+1$ we easily see $f(C_j) = u(C_j)$ for $C_j \in D_0$.

From the orthogonality in Lemma 3.6 and (3.3) we have

$$\mathcal{E}_{F_n}(f, f) = \frac{1}{4}\mathcal{E}_n(v) \sum_{j \in \Lambda'''} (z_{j+1} + z_j)^2 + \frac{1}{4}\mathcal{E}_n(w) \sum_{j \in \Lambda'''} (z_{j+1} - z_j)^2 \leq (\mathcal{E}_n(v) + \mathcal{E}_n(w)) \sum_j z_j^2$$

where we used $(z_{j+1} \pm z_j)^2 \leq 2z_{j+1}^2 + 2z_j^2$. The remaining part of the asserted energy bound is from (3.5).

Finally, suppose there is $j \in \{0, N, 3N-1\}$ for which $f(C_{j+1}) = f(C_j)$. Then $z_{j+1} = z_j$, and on the edge $L_j \cap F_n$ we have $f = u(0) - (z_{j+1} + z_j)v^j$. However (3.1) says v^j comes from the restriction of u_n to L_0 , where $u_n \equiv 1$, so v^j is constant on $L_j \cap F_n$ and so is f . \square

4. BOUNDS

Our main resistance estimate is obtained from the results of the previous sections by constructing a feasible current and potential on F_{m+n} . We use the optimal current on G_m and optimal potential on D_m to define boundary data on m -cells that are copies of F_n , and then build matching currents and potentials from Propositions 3.8 and 3.10 to prove the following theorem.

Theorem 4.1. *For $n \geq 0$ and $m \geq 1$*

$$\frac{9}{44N}R_0^{-1}R_nR_m \leq R_{m+n} \leq \frac{44N}{9}R_0^{-1}R_nR_m.$$

Proof. For fixed $m \geq 1$ let \tilde{I}_m^G be the optimal current on the graph G_m and \tilde{u}_m^D be the optimal potential on the graph D_m , both for the sets A_m and B_m . Recall that for each cell we have an address $w = w_1 \cdots w_m$ and a map ψ_w as in Section 3.1 so that $\tilde{I}_m^G \circ \psi_w$ is a current on G_0 and $\tilde{u}_m^D \circ \psi_w$ is a potential on D_0 .

Now fix $n \geq 0$ and consider F_{m+n} . Then ψ_w maps F_n to the m -cell of F_{m+n} with address w , and we write J_w for the current from Proposition 3.8 with fluxes from $\tilde{I}_m^G \circ \psi_w$ and f_w for the potential from Proposition 3.10 with boundary data from $\tilde{u}_m^D \circ \psi_w$. In particular, summing over all words of length m we have from these propositions and the optimality of the current and potential that

$$(4.1) \quad E_{F_{m+n}}\left(\sum_w J_w, \sum_w J_w\right) = \sum_w E_{F_n}(J_w, J_w) \leq \frac{11}{9}N^2 R_n E_{G_m}(\tilde{I}_m^G, \tilde{I}_m^G) = \frac{11}{9}N^2 R_n R_m^G$$

$$(4.2) \quad \mathcal{E}_{F_{m+n}}\left(\sum_w f_w, \sum_w f_w\right) = \sum_w \mathcal{E}_{F_n}(f_w, f_w) \leq \frac{2}{N}R_n^{-1} \mathcal{E}_{D_m}(\tilde{u}_m^D, \tilde{u}_m^D) = \frac{2}{N}R_n^{-1}(R_m^D)^{-1}.$$

Since \tilde{I}_m^G is a current, its flux through the edges incident at a non-boundary point is zero. Using this fact at the vertex on the center of a side where two m -cells meet we see that the net flux of $\sum_w J_w$ through such a side is zero. Moreover, in $\sum_w J_w$ the flux through this side is a (scaled) copy of v^j from (3.1). Using the fact that v^j is a rotate of v^0 and $v^0(\bar{z}) = v^0(z)$, we see that all the fluxes are multiples of a single vector field, and thus the cancellation of the net flux guarantees cancellation of the fluxes themselves. By the same argument used in proving Lemma 3.7 we conclude that $\sum_w J_w$ is a current on F_{m+n} . Its net flux through a boundary edge is the same as that of \tilde{I}_m^G , so is -1 through A_{m+n} and 1 through B_{m+n} . Hence $\sum_w J_w$ is a feasible current from A_{m+n} to B_{m+n} on F_{m+n} , and (4.1) together with Theorem 2.3 implies

$$(4.3) \quad R_{m+n} \leq E_{F_{m+n}}\left(\sum_w J_w, \sum_w J_w\right) \leq \frac{11}{9}N^2 R_n R_m^G.$$

Similarly, we can see that $\sum_w f_w$ extends by continuity to give a potential on F_{m+n} . Each side where two m -cells meet is the line segment at the intersection of the closures of copies of triangles T_j and $T_{j'}$ under maps $\psi_w, \psi_{w'}$ corresponding to the m -cells. Extending $\sum_w f_w$ to the closure of each of these triangles we see it coincides with \tilde{u}_m^D at the endpoints of this line segment, while along the line it is a linear combination of v^j and w^j as in Proposition 3.10. This linear combination

depends only on the endpoint values, so is the same on the line from $\psi_w(T_j)$ as on the line from $\psi_{w'}(T_{j'})$, showing that $\sum_w f_w$ has continuous extension to F_{m+n} . Since \tilde{u}_m^D is 0 at all endpoints of sides of cells in A_{m+n} and 1 at all endpoints of sides in B_{m+n} , the final result of Proposition 3.10 ensures $\sum_w f_w$ has value 0 on A_{m+n} and 1 on B_{m+n} , so is a feasible potential. Combining this with (4.2) and (2.2) gives

$$(4.4) \quad R_{m+n}^{-1} \leq \mathcal{E}_{F_{m+n}} \left(\sum_w f_w, \sum_w f_w \right) \leq \frac{2}{N} R_n^{-1} (R_m^D)^{-1}.$$

Our estimates (4.3) and (4.4), together with Lemma 3.3, give for $n \geq 0$, $m \geq 1$ that

$$\frac{N}{2} R_n R_m^D \leq R_{m+n} \leq \frac{11}{9} N^2 R_n R_m^G = \frac{22}{9} N^2 R_n R_m^D.$$

In particular, for $n = 0$ we have $R_m^D \leq \frac{2}{N} R_0^{-1} R_m$ and $\frac{9}{22N^2} R_0^{-1} R_m \leq R_m^D$, which may be substituted into the previous expression to obtain the theorem. \square

REFERENCES

- [1] Ulysses A. IV Andrews. *Existence of Diffusions on $4N$ Carpets*. PhD thesis, University of Connecticut, 2017. <https://opencommons.uconn.edu/dissertations/1477>.
- [2] M. T. Barlow and R. F. Bass. On the resistance of the Sierpiński carpet. *Proc. Roy. Soc. London Ser. A*, 431(1882):345–360, 1990.
- [3] M. T. Barlow, R. F. Bass, and J. D. Sherwood. Resistance and spectral dimension of Sierpiński carpets. *J. Phys. A*, 23(6):L253–L258, 1990.
- [4] Russell Brown. The mixed problem for Laplace’s equation in a class of Lipschitz domains. *Comm. Partial Differential Equations*, 19(7-8):1217–1233, 1994.
- [5] Peter G. Doyle and J. Laurie Snell. *Random walks and electric networks*, volume 22 of *Carus Mathematical Monographs*. Mathematical Association of America, Washington, DC, 1984.
- [6] Lawrence C. Evans and Ronald F. Gariepy. *Measure theory and fine properties of functions*. Studies in Advanced Mathematics. CRC Press, Boca Raton, FL, 1992.
- [7] Pierre Grisvard. *Elliptic problems in nonsmooth domains*, volume 69 of *Classics in Applied Mathematics*. Society for Industrial and Applied Mathematics (SIAM), Philadelphia, PA, 2011.
- [8] John E. Hutchinson. Fractals and self-similarity. *Indiana Univ. Math. J.*, 30(5):713–747, 1981.
- [9] William P. Ziemer. *Weakly differentiable functions*, volume 120 of *Graduate Texts in Mathematics*. Springer-Verlag, New York, 1989. Sobolev spaces and functions of bounded variation.

CLAIRE CANNER, ROCHESTER INSTITUTE OF TECHNOLOGY
Email address: clairemcanner@gmail.com

CHRISTOPHER HAYES, DEPARTMENT OF MATHEMATICS, UNIVERSITY OF CONNECTICUT, STORRS, CT 06269-1009, U.S.A.
Email address: christopher.k.hayes@uconn.edu

SHINYU HUANG, WILLIAMS COLLEGE
Email address: wsh10@williams.edu

MICHAEL ORWIN, KALAMAZOO COLLEGE
Email address: orwinmc@gmail.com

LUKE G. ROGERS, DEPARTMENT OF MATHEMATICS, UNIVERSITY OF CONNECTICUT, STORRS, CT 06269-1009, U.S.A.
Email address: luke.rogers@uconn.edu